SERI/TP-217-3223
UC Category: 60
DE88001109

Accurate Rotor Loads Prediction Using the FLAP Dynamics Code

A.D. Wright
R.W. Thresher

October 1987

Prepared for Windpower '87
San Francisco, California
5-8 October, 1987

Prepared under Task No. 4845.300

Solar Energy Research Institute
A Division of Midwest Research Institute

1617 Cole Boulevard
Golden, Colorado 80401-3393

Prepared for the
U.S. Department of Energy
Contract No. DE-AC02-83CH10093

Printed in the United States of America
Available from:
National Technical Information Service
U.S. Department of Commerce
5285 Port Royal Road
Springfield, VA 22161

Price: Microfiche **A01**
Printed Copy **A02**

Codes are used for pricing all publications. The code is determined by the number of pages in the publication. Information pertaining to the pricing codes can be found in the current issue of the following publications, which are generally available in most libraries: *Energy Research Abstracts, (ERA); Government Reports Announcements* and Index (*GRA* and I); *Scientific and Technical Abstract Reports (STAR);* and publication, NTIS-PR-360 available from NTIS at the above address.

SERI

ACCURATE ROTOR LOADS PREDICTION USING THE FLAP DYNAMICS CODE

A. D. Wright
R. W. Thresher
Solar Energy Research Institute
1617 Cole Blvd., Golden, Colo., 80401

ABSTRACT

Accurately predicting wind turbine blade loads and response is very important in predicting the fatigue life of wind turbines. There is a clear need in the wind turbine community for validated and user-friendly structural dynamics codes for predicting blade loads and response. At the Solar Energy Research Institute (SERI), a Force and Loads Analysis Program (FLAP) has been refined and validated and is ready for general use.

Currently, FLAP is operational on an IBM-PC compatible computer and can be used to analyze both rigid- and teetering-hub configurations. The results of this paper show that FLAP can be used to accurately predict the deterministic loads for rigid-hub rotors.

This paper compares analytical predictions to field test measurements for a three-bladed, upwind turbine with a rigid-hub configuration. The deterministic loads predicted by FLAP are compared with 10-min azimuth averages of blade root flapwise bending moments for different wind speeds.

INTRODUCTION

Past comparisons of wind turbine rotor load predictions with field test data have indicated large discrepancies. For example, Figure 1 (taken from [1]) illustrates the significant underprediction of Boeing MOD-2 root bending moments when comparing field test measurements with computations obtained using FLAP (this is described in [2]). These large discrepancies are thought to be due to turbulence fluctuations and the fact that the mean inflow to the rotor disk is unknown.

To compare predictions to test measurements for a case where the turbulence levels were low and the inflow was well known, FLAP code predictions were compared to measurements taken from a 1/20-scale model of the Boeing MOD-2 tested in a wind tunnel [3]. In the wind tunnel test, the wind-shear profiles were accurately measured after having been created by wire mesh screens set up in the tunnel [4]. The 1/20-scale model was tested in both the teetering- and rigid-hub configurations at different wind speeds.

It was shown in [3] that the correct representation of the wind-shear distribution (inflow) was important for accurately determining the cyclic flapwise bending moments for both the rigid- and teetering-hub cases. Using just the simple power-law wind shear was shown to be inadequate for accurately predicting the blade cyclic flapwise bending loads.

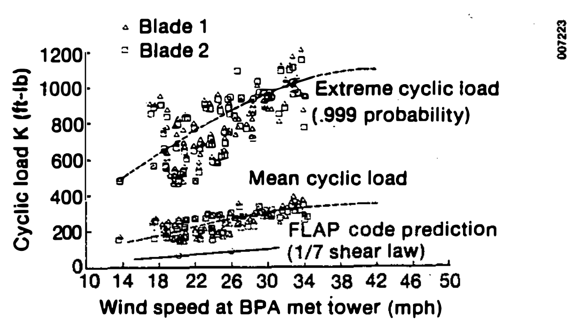

Figure 1. **CYCLIC FLAPWISE MOMENTS AT BLADE STATION 370 (UNIT #2, 70% VG, FROM [1])**

Having confirmed the code's ability to predict loads and forces from wind tunnel measurements, the next step was to compare the prediction of the FLAP code with field test measurements from a full-scale turbine. The forces acting on a wind turbine operating in atmospheric winds must be separated into deterministic and stochastic components. The deterministic forces are caused by the steady portion of the wind loading, the centrifugal forces, and gravity-induced loads. These deterministic forces have both steady components and cyclic components. The cyclic components are caused by the steady wind gradient across the rotor disk, the tower shadow, gravity acting on the rotating blades, and yaw misalignment of the turbine. Wind turbulence causes the random stochastic portion of the turbine loads. Turbulent wind varies as a function of time and space and imposes a randomly varying aerodynamic load on the rotor.

This paper describes the comparison of FLAP predictions with the deterministic forces computed from the field test measurements. It is assumed that for stationary operating conditions of the test turbine the deterministic and stochastic loads can be separated by the process of azimuth averaging. Azimuth averaging is accomplished by binning the measured forces with respect to the azimuth angle of the rotor blade for a large number of rotor cycles. The results of this averaging process are signals that are periodic with rotor angle and provide an estimate of the deterministic forces acting over the averaging time. The stochastic forces are then given by subtracting the azimuth-averaged signals from the original signals. A comparison of FLAP predictions for the stochastic forces remains for investigation in the near future. Unless FLAP can adequately predict the deterministic loads, there is little reason to expect an accurate prediction of the turbulence-induced loads.

TURBINE DESCRIPTION

As part of the DOE Cooperative Field Test Program, SERI and Southern California Edison (SCE) carried out a comprehensive field measurement program on the SCE-owned, 330-kW, horizontal-axis wind turbine located near Palm Springs, California, in San Gorgonio Pass. The measurement program included a complement of structural load measurements to characterize the dynamic response of the turbine, as well as an array of wind sensors to characterize both the mean and turbulent wind field in front of the turbine.

The field test turbine, manufactured by James Howden and Company, was a three-bladed, upwind machine with a rigid hub and wood/epoxy blades. It was rated at 330 kW in a hub-height wind speed of 32.4 mph (14.5 m/s) and was designed to operate in cut-in and cut-out wind speeds of 13.4 and 62.6 mph (6.0 and 28.0 m/s), respectively. The rotor diameter was 85.3 ft (26 m) and the rotor speed was 42 rpm. The blades were tapered and twisted, with a maximum chord of 4.8 ft (1.47 m) and a maximum twist angle of 16°; the blade tapered to a 2.6-ft (0.8-m) chord and 0° twist at the blade tip. The blade airfoil section was a GA(W)-1, 17% thick. The blade dimensions are shown in Table 1.

The rotor axis centerline above the ground was at 79.1 ft (24.1 m), and the rotor coning angle (precone) was 0°. The tower diameter was 5.9 ft (1.8 m), and the distance from the yaw axis to the rotor plane was 11.5 ft (3.5 m). Figure 2 is a sketch of the turbine.

THE INSTRUMENTATION

A total of 44 channels of data were recorded in multiplexed form on a Honeywell 101 14-channel tape recorder. Thirteen channels of machine data were

Table 1. **HOWDEN WIND TURBINE BLADE DIMENSIONS**
(From [5])

Radius (ft)	Chord (ft)	Twist* (deg.)	Notes
1.31	2.10	16.0	Root (fixed pitch)
9.84	4.80	16.0	Blade "knee"
36.10	3.10	3.2	Tip joint
42.60	2.60	0.0	Tip (pitchable)

*Toward feather.

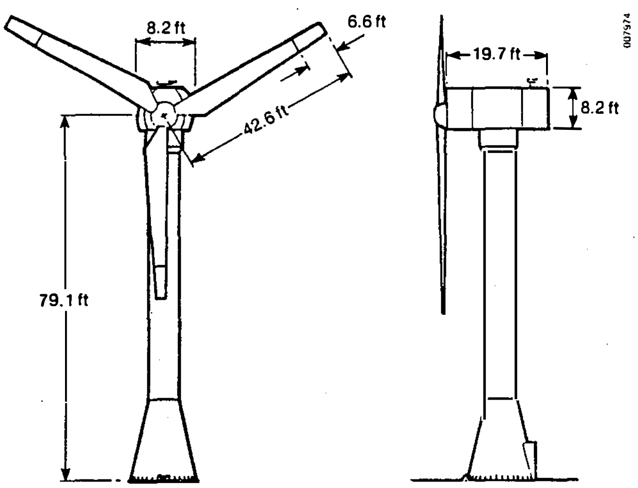

Figure 2. **THE HOWDEN HWP 330/26 WIND TURBINE (FROM [5])**

collected through the Howden data system. The effective cut-off frequency of the Howden data system was about 30 Hz. The 31 channels of atmospheric data were low-pass filtered at 10 Hz. The wind data of interest for this study came from the vertical-plane array using three-axis UVW Gill propeller anemometers located 68.9 ft (21 m) [or 0.8 rotor diameters (D)] due west and upwind of the turbine in the prevailing wind direction. The numbering scheme for the anemometers on this array is shown in Figure 3. In addition, there was a single

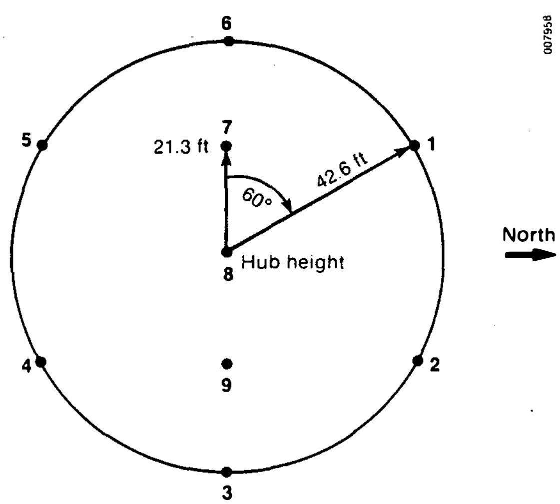

Figure 3. **PLACEMENT AND NUMBERING OF THE UVW GILL ANEMOMETERS ON THE ARRAY (LOOKING UPWIND TO THE WEST)**

UVW Gill propeller anemometer at hub height, located 2D upwind. The only machine data used for this study was the blade-root bending moment at the 4.9-ft (1.5-m) spanwise station. The analog data collected during the test were digitized at SERI using the NEFF 720 system at a sample rate of 41.67 Hz. This high rate was necessary to accurately resolve the blade angular position for azimuth averaging.

THE FLAP MODEL

The FLAP code requires the usual geometric blade properties, such as the twist and taper described in Table 1. In addition, the operating conditions such as rotor speed, wind speed, wind-shear gradient, and yaw angle are required. The code uses a very simple, linear, quasi-steady aerodynamic model. Only the lift curve slope, a maximum lift coefficient, and a drag coefficient are essential. However, these coefficients can be varied along the span to improve the modeling accuracy. The lift curve for the GA(W)-1 airfoil is shown in Figure 4.

To model the dynamic response of the blade, the distributed weight of the blade and the stiffness distribution are the key parameters. These distributions are plotted in Figure 5. To obtain good predictive capabilities with any type of dynamic model, the natural frequencies of the model must

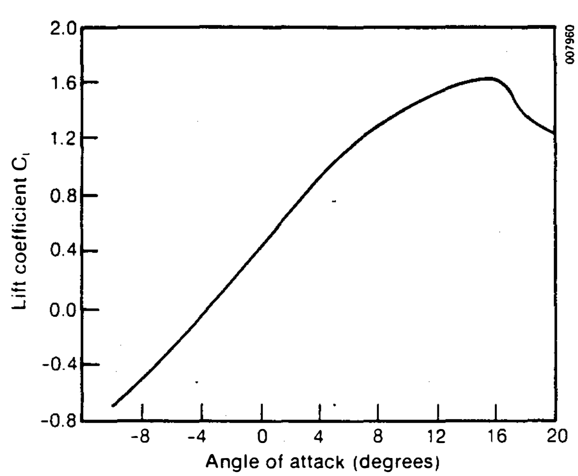

Figure 4. **LIFT CURVE FOR THE GA(W)-1 AIRFOIL**

SERI

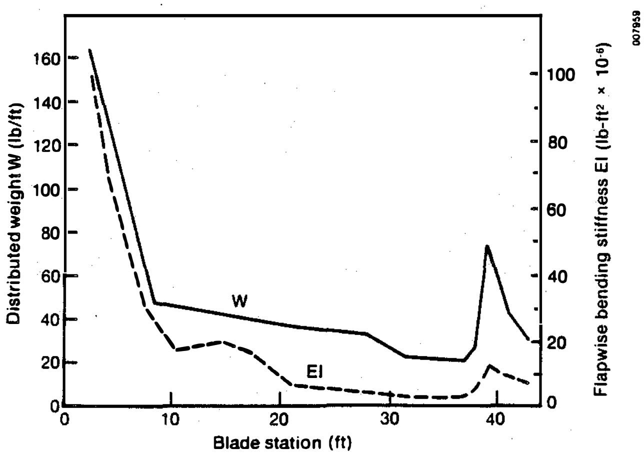

Figure 5. WEIGHT AND STIFFNESS DISTRIBUTION FOR THE HOWDEN 42.6-ft WOOD/EPOXY BLADE

faithfully reproduce those of the physical structure. Otherwise, the dynamic response errors will be quite large. The predicted natural frequencies for the turbine are listed in Table 2 as computed by Howden [5].

Table 2 shows that there are several natural frequencies quite close to a frequency of two times the rotor passage frequency (or 2P). FLAP does not account for tower motion; thus, it was impossible to model the actual blade/tower interactions of the turbine. To make a simple approximation for this situation, only one blade mode was used to model the blade flapping response, and the frequency was set at 1.40 Hz (2P). This covered the closely spaced natural frequencies near 1.40 Hz and disregarded the higher frequencies.

The mass and stiffness distributions of Figure 5 were used as a starting approximation. Then, the

Table 2. PREDICTED NATURAL FREQUENCIES (NONROTATING)

Mode	Frequency Hz	Frequency Per rev.	Mode Shape
1	1.33	1.90	Rotor flap - tower (fore to aft)
2	1.43	2.04	Rotor flap (no tower)
3	1.44	2.04	Rotor flap (no tower)
4	1.53	2.20	Tower - rotor side-to-side
5	1.72	2.50	Rotor flap - tower (fore to aft)
6	3.43	4.90	Blade flap

resulting modal stiffness coefficient computed by the FLAP code was manually adjusted to set the blade rotating natural frequency right on 1.40 Hz (2P). The modal mass coefficients were not adjusted because that would have changed the centrifugal loads on the rotor.

Even though this machine had a tip-controlled blade, time-series segments were chosen in which the pitch angles of the tip region were close to 0° to simplify the analysis. Thus, neither the twist distribution nor the pitch angle of the blade was modified to account for small pitch changes near the tip.

THE DETERMINISTIC WIND INFLOW CALCULATIONS

In this paper, FLAP code predictions are compared to blade load test measurements for four different 10-min data cases. These data cases had different wind speeds, turbulence intensities, and yaw errors, although only case #4 had a large yaw angle. The blade tip pitch angles were small and neglected. Table 3 shows the different conditions for the four cases.

The mean wind inflow to the turbine was determined by computing the mean velocity at each anemometer location for each 10-min data case. These 10-min means are plotted in Figure 6 as a function of natural logarithm (ln) of height above the ground. The hub-height anemometer located 2D upwind of the

Table 3. OPERATING CONDITIONS FOR THE FOUR 10-MINUTE DATA CASES USED FOR COMPARISON

	Case Number 1	2	3	4
Wind speed (ft/s)*	31.50	41.70	34.84	43.60
Turbulence intensity	0.13	0.13	0.18	0.12
Yaw error (deg.)	2.40	0.50	3.90	-14.00
Tip position (deg.)	0.26	0.50	0.02	0.66

*The average of the 9 anemometers, V2 to V10.

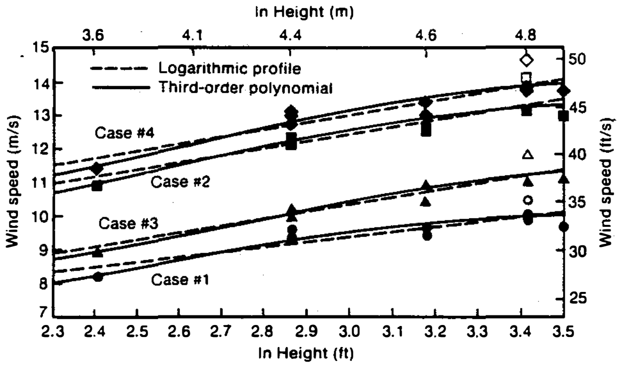

Figure 6. MEAN INFLOW TO THE ROTOR FOR THE FOUR 10-MINUTE DATA CASES

turbine was included in this plot. Anemometer #1 can be identified as the unfilled symbol in this plot and can be seen as consistently high. For this reason, it was dropped from the subsequent calculations. The wind profile for each case was curve-fit to a logarithmic profile (equivalent to the power law), which is shown as the dashed line. In addition, the profile was fit to a simple cubic polynomial in height. The cubic polynomial does better at fitting the velocity profile near the ground, which will later be shown to be important for accurately predicting the 2P cyclic bending moments. Higher-order curve fits to the velocity profile could have been used, but the low-order fit helps to average out measurement errors.

As a first approximation to the deterministic wind excitation, the familiar power law wind-shear profile (equivalent to the logarithmic profile) was used as the shear excitation for FLAP. This relationship can be expressed as

$$V(z) = V_{ref}(1 + z/h)^m , \quad (1)$$

where z is height (equal to zero at hub height), h is hub height, V_{ref} is the disk averaged wind speed (obtained by averaging all of the wind speeds for the 10-min data cases), and m is the power-law wind-shear coefficient determined by curve-fitting the data of Figure 6.

Next, for a better approximation, the 3rd-order polynomial fit to the wind speed data was used as the wind-shear excitation to FLAP. The expression was written in the form

$$V(z) = A_0 + A_1 z + A_2 z^2 + A_3 z^3 . \quad (2)$$

Substituting $z = r\cos\psi$ transformed this equation into blade coordinates, resulting in the expression

$$v(r,\psi) = (A_0 + 0.5A_2r^2) + (A_1r + 0.75A_3r^3)\cos\psi + (0.5A_2r^2)\cos 2\psi + (0.25A_3r^3)\cos 3\psi . \quad (3)$$

This expression, when introduced as the rotor excitation for the wind shear, gives more excitation for the 2P harmonic than does the power-law profile.

THE DETERMINISTIC ROOT-BENDING MOMENT CALCULATIONS

The azimuth-averaged root-bending moment was computed by binning the raw time-series data on blade azimuth angle for the full 10-min data case (420 revolutions).

Harmonics of the azimuth-averaged bending moment data were computed by fitting a Fourier series as a function of the blade azimuth angle. Such a series takes the form

$$M(\psi) = M_0 + M_{1c}\cos\psi + M_{1s}\sin\psi + M_{2c}\cos 2\psi + M_{2s}\sin 2\psi + \ldots , \quad (4)$$

where M is the flapwise bending moment and ψ is the blade angular position (with $\psi = 0$ indicating the straight-up position). The coefficients M_{nc} and M_{ns} define the magnitude of the harmonic content of the flapwise bending response, while M_0 denotes the steady or mean term. For the comparisons made in this paper, the magnitude of the nth harmonic is defined as

$$M_n = (M_{nc}^2 + M_{ns}^2)^{1/2} . \quad (5)$$

Figures 7 and 8 show the comparison of FLAP predicted harmonics to the harmonics of the 10-min azimuth-averaged blade data for comparison cases

SERI

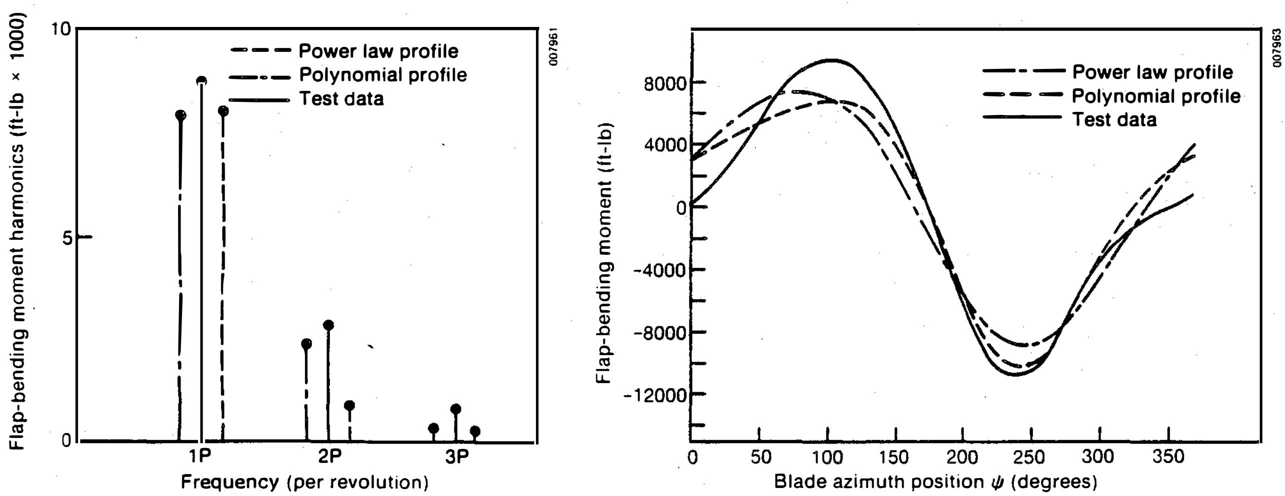

Figure 7. COMPARISON OF HARMONIC CONTENT AND WAVEFORM FOR PREDICTIONS AND EXPERIMENTAL MEASUREMENTS FOR CASE #1

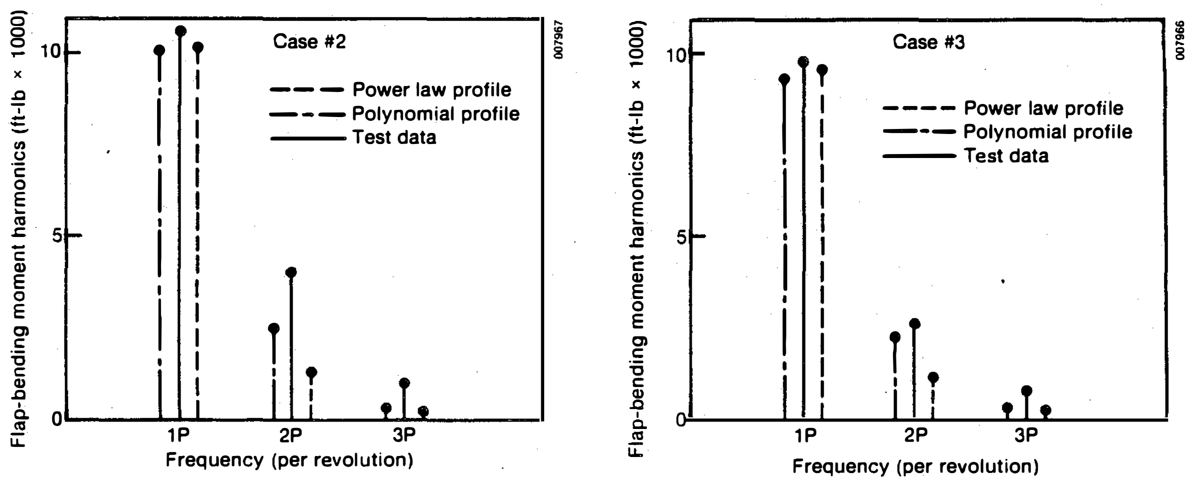

Figure 8. COMPARISON OF HARMONIC CONTENT FOR PREDICTIONS AND EXPERIMENTAL MEASUREMENTS FOR CASES #2 AND #3

#1-#3. Using the power-law wind-shear profile caused the underprediction of the 2P harmonics by 70% in some cases, while using the 3rd-order polynomial resulted in a smaller error (about 20%). Both profiles gave fairly good approximations for the 1P harmonic. Figure 7 also shows the resulting waveform of the FLAP predictions compared to the azimuth-averaged blade measurement waveform for case #1. The waveforms for the other cases exhibit similar behavior. A small amount of tower shadow was used in the FLAP code to simulate the wind flow around the tower, although the effects on the cyclic bending moments are predominantly due to the wind-shear profile.

Data case #4 had a significant yaw error (-14°). Figure 9 shows the comparison of FLAP predicted harmonics and harmonics of the azimuth-averaged test data. The magnitude of the 1P harmonic for the test data is the highest for this data case. The prediction of the 1P harmonic is significantly underestimated for this case, whereas in all of the other cases the FLAP code gave reasonable estimates for this harmonic.

Figure 9 also shows the waveform of the FLAP prediction plotted against the waveform of the azimuth-averaged data for this case. In this case, the 3rd-order polynomial was used as the shear in-

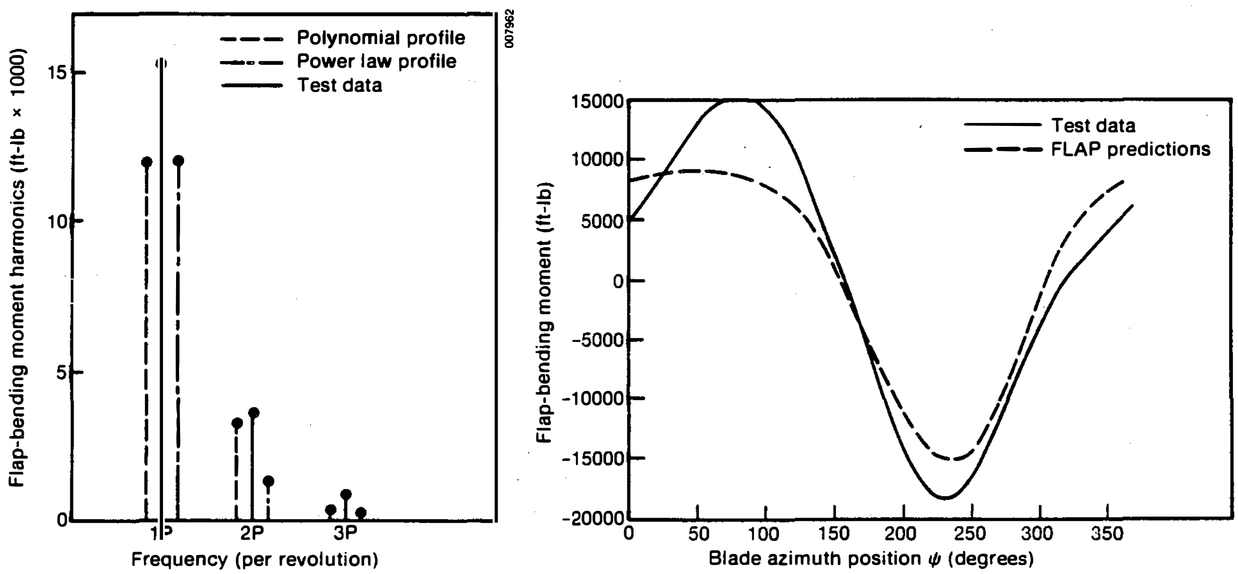

Figure 9. COMPARISON OF HARMONIC CONTENT AND WAVEFORM FOR PREDICTIONS AND EXPERIMENTAL MEASUREMENTS FOR CASE #4 (YAW ERROR = -14°)

put. The greatest discrepancies between predicted results and the measured waveform occurs when the blade is near 90° azimuth angle (with the blade horizontal). This could be caused by inaccuracies in the induced velocity calculation for the yawed flow case, or possibly by dynamic stall.

The reasons for this discrepancy are being investigated with the hope of improving the FLAP code calculations for yawed flow cases. Other data cases for this machine containing a high yaw error will be analyzed and compared to FLAP predictions before any code modifications are made. The induced flow calculations for yawed flow conditions will be reviewed and possibly revised in the FLAP code.

CONCLUSIONS

Flap code predictions were compared to azimuth-averaged flap-bending moments at the 4.9-ft (1.5-m) station for this machine. It has been demonstrated that the FLAP code can predict the deterministic portion of the loading quite well, provided the inflow mean shear profile is closely approximated and the yaw errors are small.

The FLAP code can now be used with confidence that the deterministic loads can be accurately estimated for design purposes. A revised, updated, and better-documented form of the code is now being released for use on personal computers. A full description of the code, with a user's manual, is soon to be released [6].

A first step in rotor load prediction for a field test turbine has now been concluded by assuring that FLAP can accurately predict the deterministic loads for a field test turbine. This was a necessary step before proceeding to the more difficult task of adding the effects of turbulent wind fluctuations to FLAP. Now, the task of including the turbulence-response calculation is beginning.

ACKNOWLEDGEMENTS

This work could not have been accomplished without the efforts of Susan Hock and Greg Hampsen of SERI, who made valuable contributions in analyzing and interpreting the machine test data. They prepared the test data for a direct comparison to code predictions. Also, thanks must be extended to Tom Hausfeld, formerly with SERI, for his many weeks of work at the test site to collect this valuable data. His careful test engineering work made the data from the Howden turbine described in this paper available to SERI and other researchers.

REFERENCES

1. Bovarnick, M.L., Shipley, S.A., and Finger, R.W., "Goodnoe Hills MOD-2 Cluster Test Program," AP-4060, Vol. 2, Electric Power Research Institute, Palo Alto, Calif., May 1985.

2. Thresher, R.W., Wright, A.D., and Hershberg, E.L., "A Computer Analysis of Wind Turbine Blade Dynamic Loads," Journal of Solar Energy Engineering, 108, (Feb. 1986), pp. 17-25.

3. Wright, A.D., and Thresher, R.W., "A Comparison of Predicted Wind Turbine Blade Loads to Test Measurements," SERI/TP-217-3070, presented at the Sixth ASME Wind Energy Symposium, Dallas, Tex., Feb. 16-18, 1987.

4. Shipley, S.A., "Wind Tunnel Test, WTS MOD-2, Full Span Control, 1/20th Scale Model," nonpublished report on wind tunnel experiment, Code IDENT. No. 81205 D277-10129-1, Boeing Aerospace Company, Seattle, Wash.

5. Redmond, I., Anderson, C.G., and Jamieson, P., "Dynamic Response of a 330kW Horizontal Axis Wind Turbine Generator," nonpublished report by James Howden and Co. LTD, under SERI cooperative agreement No. DE-FC02-85CH10249.

6. Wright, A.D., Buhl, M.L., and Thresher, R.W., "FLAP Code Development and Validation," SERI/TR-217-3125, Solar Energy Research Institute, Golden, Colo.